PCCP

PAPER

View Article Online
View Journal | View Issue

Cite this: *Phys. Chem. Chem. Phys.*, 2016, **18**, 30484

Ultrafast ion migration in hybrid perovskite polycrystalline thin films under light and suppression in single crystals†

Jie Xing,‡[ab] Qi Wang,‡[a] Qingfeng Dong,[a] Yongbo Yuan,[ac] Yanjun Fang[a] and Jinsong Huang*[a]

Received 21st September 2016,
Accepted 13th October 2016

DOI: 10.1039/c6cp06496e

www.rsc.org/pccp

Understanding the influence of light on ion migration in organic–inorganic halide perovskite (OIHP) materials is important to understand the photostability of perovskite solar cells. We reveal that light could greatly reduce the ion migration energy barrier in both polycrystalline and single crystalline OIHP. The activation energies derived from conductivity measurement under 0.25 Sun decrease to less than one half of the values in the dark. A typical ion drift velocity in $CH_3NH_3PbI_3$ polycrystalline films is 1.2 μm s^{-1} under 1 Sun, compared with 0.016 μm s^{-1} under 0.02 Sun. Ion migration across the photoactive layers in most OIHP devices thus takes only subseconds under 1 Sun illumination, which is much shorter than what it was thought to take. Most important of all, ion migration through a single crystal surface is still too slow to be observed even after illumination for two days due to the large ion diffusion activation energy, >0.38 eV.

Introduction

Organic–inorganic halide perovskites (OIHPs) have attracted tremendous research interest in the photovoltaic community due to their extraordinarily long carrier recombination lifetime, much longer carrier diffusion length than optical film thickness, *etc.*[1–5] These superior optoelectronic properties have driven the skyrocketing of the power conversion efficiency of perovskite solar cells from 3.8% to over 22% in the past few years.[6,7] Among all the intriguing properties of OIHPs, the presence of ion-migration has gained broad attention due to the presence of photocurrent hysteresis in many OIHP solar cells.[8] Ion migration has also been speculated to correlate with many unique phenomena observed in OIHP materials, such as switchable photovoltaics,[9] the photo-induced poling effect,[10] light-induced phase separation,[11] a giant dielectric constant[12] and self-healing.[13,14] To reveal how fast the ion migration occurs in polycrystalline $CH_3NH_3PbI_3$ (or $MAPbI_3$), we previously measured the Arrhenius plot of conductivity, and an activation energy of $\sim$0.3 eV in $MAPbI_3$ was derived,[15] which has also been widely acknowledged as a typical value obtained by both experimental and theoretical results of other groups.[16–18] Very recently, an interesting phenomenon called photostriction revealed the very strong lattice-phonon coupling in $MAPbI_3$.[19] In our previous study, we observed that non-optimized devices with a small open circuit voltage (V_{OC}) could be self-poled by a photovoltage induced additional electric field, which is much more significant under strong light illumination.[10] These new observations lead us to consider that illumination light might also stimulate ion migration and so ions in real operating devices could be much easier to move than they were previously thought to be.

Here we studied the influence of light on ion migration by directly measuring the activation energy of ion conduction in both polycrystalline films and single crystals in the dark and under illumination conditions. It has been found that ion migration could be significantly enhanced by sunlight illumination in polycrystalline films, while the activation energy in single crystals is still too large for notable ion migration to occur.

We first illustrate the impact of light illumination on ion migration by a poling experiment on a lateral structure device. We previously demonstrated that, in lateral structure devices, the formation of a PbI_2 thread and a reversible conversion between PbI_2 and $MAPbI_3$ could be observed under an optical microscope at an elevated temperature of 330 K.[20] The speed of the PbI_2 thread motion directly reflects the ion migration velocity, because the motion of this PbI_2 thread is mediated by both I^- and MA^+ (vacancies) migration. Therefore this provides

[a] *Department of Mechanical and Materials Engineering, University of Nebraska-Lincoln, Lincoln, 68588, NE, USA. E-mail: jhuang2@unl.edu*
[b] *School of Science, China University of Geosciences, Beijing, 100083, P. R. China*
[c] *Hunan Key Laboratory of Super Microstructure and Ultrafast Process, School of Physics and Electronics, Central South University, Changsha, Hunan 410083, P. R. China*

† Electronic supplementary information (ESI) available. See DOI: 10.1039/c6cp06496e
‡ J. X. and Q. W. contributed to this work equally.

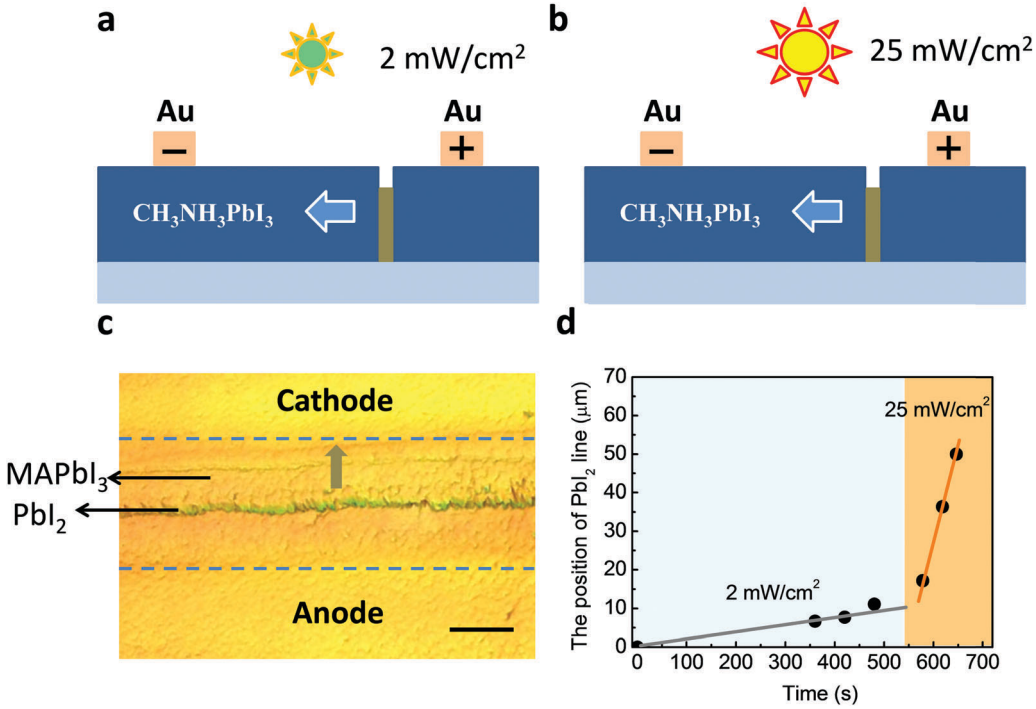

Fig. 1 The formation and movement of the PbI_2 thread in $MAPbI_3$ under light and bias at 330 K. (a and b) A schematic illustration of the cross section of the lateral structure device under light (2 mW cm^{-2} for a and 25 mW cm^{-2} for b) and bias (4 V μm^{-1}). (c) A laser confocal scanning microscopy image of the $MAPbI_3$ film with the PbI_2 thread. The scale bar is 25 μm. (d) The position of the PbI_2 thread at different times under illumination of different light intensities.

a platform to directly observe the influence of light on the ion migration velocity. We used a $MAPbI_3$ film formed on glass with a small grain size of 300 nm for this study. A schematic illustration of the lateral device is shown in Fig. 1a and b. To shorten the PbI_2 thread moving time, a large electric field of 4 V μm^{-1} was applied to the uncovered $MAPbI_3$ film at 330 K. When illuminating the $MAPbI_3$ film with a light intensity of 25 mW cm^{-2} (0.25 Sun), a PbI_2 thread appeared in about 20–30 s after turning on the poling bias. A laser confocal scanning microscopy image of the $MAPbI_3$ film with the PbI_2 line is shown in Fig. 1c. The PbI_2 thread moved continuously toward the cathode. It took ~104 s for the PbI_2 thread to cross the 50 μm spacing between the two electrodes, indicating a drift velocity of 0.48 μm s^{-1}. The corresponding ion mobility was calculated to be 1.2×10^{-9} cm^2 V^{-1} s^{-1}, which is close to Yuan's result considering that there is a small variation of quality of the polycrystalline films.[20] In contrast, when the illumination light intensity to the sample was reduced to 2 mW cm^{-2} (0.02 Sun), which is the weakest light intensity for recording a video, it took ~360 s for the PbI_2 thread to be formed near the anode and the thread moved at a very low velocity of 0.016 μm s^{-1} toward the cathode. The corresponding ion mobility is 4×10^{-11} cm^2 V^{-1} s^{-1}, which is tens of times smaller than that observed under 0.25 Sun. At the halfway point of its movement, we increased the light intensity back to 0.25 Sun, after which we immediately observed an evident expansion of the PbI_2 line and increase in its motion speed. The position of the PbI_2 thread changes with the poling time under illumination by different light intensities as shown in Fig. 1d. Video S1 of this migration process can be found in the ESI.†

The activation energy of ionic conduction directly represents how easily ions move, and thus was applied here to quantitatively characterize the influence of light illumination on ion migration.[21,22] The activation energy of ion migration was extracted from the dependence of the conductivity of the $MAPbI_3$ films on temperature. In short, we used a lateral structure device which consists of two Au electrodes deposited on $MAPbI_3$ polycrystalline films or single crystals, as illustrated in Fig. 2a. The polycrystalline films were formed by our previously developed solvent annealing method which can produce high efficiency perovskite solar cells with an efficiency of 19–21%.[23,24] Details about the device fabrication can be found in the Experimental section. Here a lateral device structure was employed in order to suppress the electronic conduction and highlight the ion conducting contribution to the total current. The atom or ion migration rate (r_m) in a solid is determined by the activation energy (E_a) by the Nernst–Einstein relation:

$$\sigma(T) = \frac{\sigma_0}{T}\exp\left(\frac{-E_a}{kT}\right) \quad (1)$$

where k is the Boltzmann constant, σ_0 is a constant, and activation energy E_a can be derived from the slope of the $\ln(\sigma T) - 1/kT$ relation. In measurement, a constant electric field of 0.2 V μm^{-1} was applied, which was set to be small to reduce the poling effect. Fig. 2b shows the total electrical conductivity of the $MAPbI_3$ film with an average grain size of ~1 μm in the dark and under

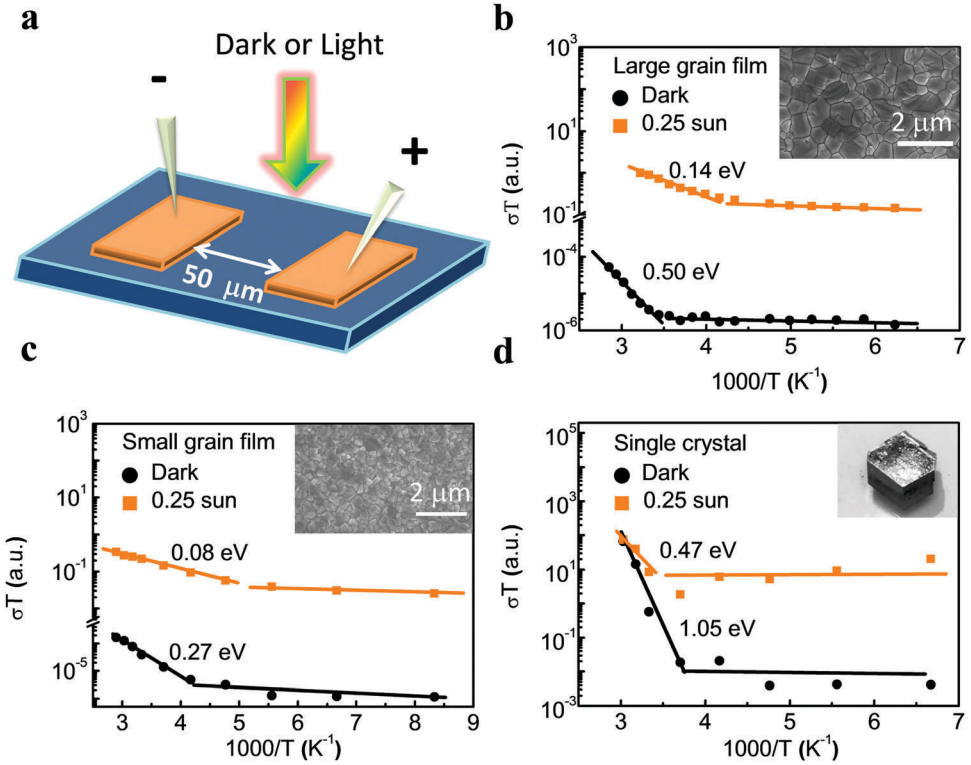

Fig. 2 Ion migration properties of $MAPbI_3$ films and single crystals. (a) A scheme of the conductivity measurement setup. The temperature-dependent conductivity of a large-grain film (b), a small-grain film (c), and a single crystal (d). The inset pictures of b–d are SEM images of the test samples.

illumination. The activation energy in the high temperature region was fitted to be 0.50 eV under the dark conditions which is consistent with many calculation results.[16–18] The activation energy reduced dramatically to 0.14 eV under 0.25 Sun illumination (25 mW cm^{-2}), quantitatively showing that ion migration is easier under light. This phenomenon had very good repeatability because all of our studied samples (over 30) showed the same degree of E_a reduction under illumination. It was also found that the threshold temperature at which ion migration begins to dominate the total current was also reduced by light illumination. Under the dark conditions, the ions started to migrate at 240 K, while the threshold temperature moved to 210 K under illumination.

The activation energy (0.50 eV) obtained in the polycrystalline $MAPbI_3$ film with an average grain size of ~1 μm was larger than our previously reported value of 0.36 eV, which is related to the different grain boundary (GB) densities. $MAPbI_3$ films with different grain sizes, including single crystals, have been used in this study. The samples we used with a large grain size were fabricated by the solvent annealing method.[25–27] To tune the grain size, we intentionally annealed the sample without solvent to minimize the perovskite grain size. The inset of Fig. 2c shows the SEM image of such a perovskite film which has smaller grains of ~0.3 μm, compared to the ~1 μm grains in the solvent-annealed perovskite films (shown in the inset of Fig. 2b). The activation energies for the small-grain film are 0.27 eV and 0.08 eV in the dark and under illumination, respectively. Both of these are smaller than the values of the large-grain film (Fig. 2b). Single crystals represent the extreme case of large grain films. The absence of grain boundaries in single crystals should give the largest energy barrier for ion migration. Fig. 2d shows that the activation energies of ion migration in single crystals are 1.05 eV in the dark and 0.47 eV under illumination, which are at least two fold larger than those of the polycrystalline films. The results confirmed that GBs make the migration easier, and light illumination also reduces the ion conducting energy barrier along GBs as well as single crystal surfaces. The fact that the crystallinity impacts significantly on the activation energy is consistent with our recent finding that ion migration in polycrystalline films mainly occurs through GBs.[28] The more open structure at GBs offers better chances to form ion migration channels with a lower energy barrier, and the role played by incident photons is still manifested at GBs.

Generally, ion migration along a free surface is easier than along a grain boundary and through the grain bulk, due to the lack of chemical bonding on one side toward air.[29] In real solar cell devices, there is no free perovskite surface, because the surfaces are covered by charge transport layers and electrodes. To understand the influence of illumination on ion migration in real operating devices, 200 nm thick poly(methyl methacrylate) (PMMA) layers were used to cover the surface of perovskite thin films with an average grain size of 300 nm to suppress surface ion migration. The conductivities of the corresponding devices are shown in Fig. 3a. The ion conducting activation energy in the dark increased from 0.27 eV to 0.48 eV when the film surface was

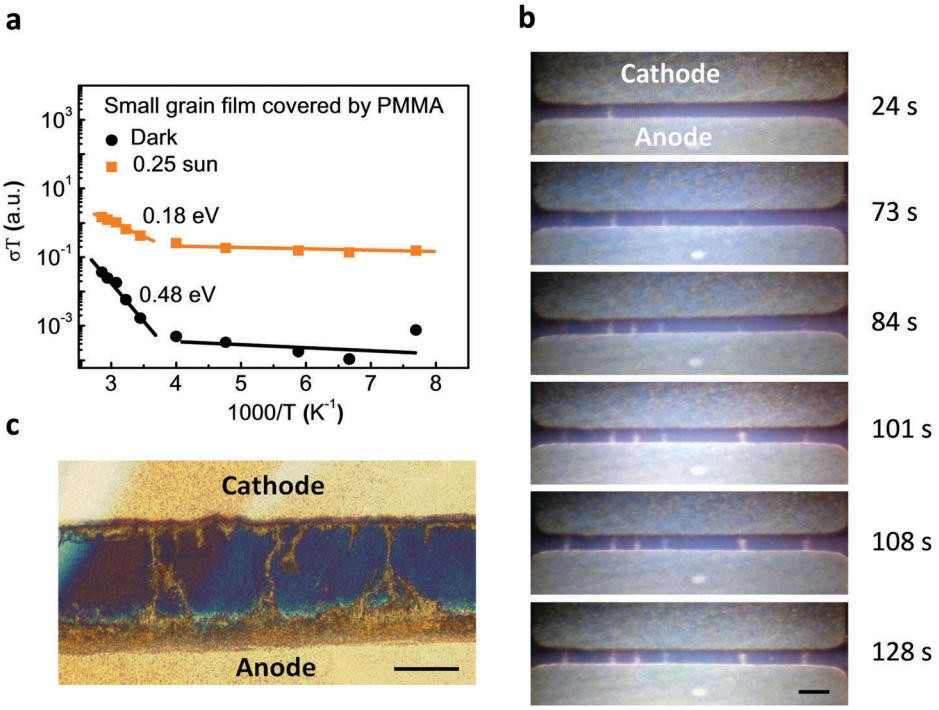

Fig. 3 Ion migration properties of small grain $MAPbI_3$ films covered by PMMA. (a) The temperature-dependent conductivity of a small-grain $MAPbI_3$ film covered by PMMA. (b) A series of snapshots of the $MAPbI_3$ film taken at different times, poling at 8 V μm^{-1} and under 0.25 Sun at 330 K. The scale bar is 100 μm. (c) A local enlarged image of the filamentary paths across the covered $MAPbI_3$ film measured by laser confocal scanning microscopy. The scale bar is 25 μm.

covered. Inferred from Shao *et al.*'s study, the activation energy measured here should still be dominated by the grain boundary migration.[28] The significantly higher ion conducting activation energy affirmed that ions moved through the grain boundary with a higher barrier than through the surface. When the device was exposed to illumination (0.25 Sun), again we got a much reduced activation energy of 0.18 eV, which is still bigger than the activation energy of the surface migration under illumination. This shows that light illumination has a significant impact on both the surface migration and grain boundary migration.

For PMMA covered $MAPbI_3$ films, ion migration became more difficult due to the absence of surface migration. We examined the poling process under illumination at 330 K, which are the same as the conditions for forming a mobile PbI_2 thread in lateral structure devices. In this case, we did not observe the formation of a PbI_2 thread for the film under illumination. In order to see visible change of the films, we had to apply a doubled field of 8 V μm^{-1} to speed up the poling process. Under 0.25 Sun illumination, several filamentary paths formed randomly between the electrodes in a time range of 130 s, as shown in Fig. 3b and c. These filaments formed at the grain boundaries and became visible under optical microscopy once massive ion migration occurred. The filaments did not form at every grain boundary, indicating that there is a variation in grain boundary openness in the polycrystalline $MAPbI_3$ films. The first filamentary path appeared at ~20 s after the poling bias was turned on. The forming process of the filamentary paths can be seen in Video S2 in ESI.† It can be seen from the video that once a filamentary channel formed, the channel spread quickly in several seconds, showing very fast ion migration/drift along the grain boundaries. It is not surprising that no change was found in the dark even when the film was poled under the high field of 8 V μm^{-1} for as long as 300 s. These results provide conclusive evidence that illumination promotes the formation of an ion migration channel and enhances the ion migration, in agreement with the measured lower activation energy under illumination. If we take an observed average channel transition time of 10 s for a rough estimation, the ion drift velocity is about 5 μm s^{-1} under an electric field of 8 V μm^{-1}. This converts to an ion mobility of 6.25×10^{-9} cm^2 V^{-1} s^{-1} which is of the same order of magnitude as that derived from the PbI_2 thread migration in the above poling study. Although the surface of the polycrystalline $MAPbI_3$ films was covered here, the comparable ion mobility with the surface ion migration indicates that some grain boundaries which formed filaments have widely open structures comparable to the film surface.

Given that the light enhanced ion migration has been established in this work, it will be important to understand what the origin of this effect is. Ion migration is a defect-mediated hopping process and the hopping rate depends on the density and position of the adjacent vacancies.[30,31] Therefore light illumination should generate more defects to facilitate ion migration. Theoretical calculations show that the decomposition energy of $MAPbI_3$ is only 0.1 eV.[32] Illumination could promote the decomposition of $MAPbI_3$ and cause more interstitial sites or vacancies, which provides more hopping opportunities for the

movable ions. Gottesman *et al.* also suggested that illumination could temper the binding between MA^+ and the PbI_6 octahedron frame.[33] Recently a large photostrictive effect (>1200 ppm) found in $MAPbI_3$ single crystals and thin films was proposed to be caused by the weakening of the hydrogen bonding by photo-carriers.[17] Despite the exact origin of the photorestriction effect being still unknown, the enlarged interatomic spacing by the photorestriction effect should generate more point defects for ion transport. However, the fact that ion migration still dominantly occurs along grain boundaries in covered perovskite thin films indicates that continuous ion migration channels, or extended defects, are needed to observe the massive ion migration.

Based on the measured ion migration rate under illumination, we can evaluate its impact in regular operating solar cells and how to suppress it. Most regular OIHP solar cells have a stronger built-in electric field of $\sim$2–3 V μm^{-1}. We can derive an ion drift velocity of 1.2 $\mu m\ s^{-1}$ with an ion mobility of $6.25 \times 10^{-9}\ cm^2\ V^{-1}\ s^{-1}$ in the polycrystalline perovskite film covered with PMMA. The transition time for ions to go through a 500 nm thick film can thus reduce to 0.4 s in regular devices, which suggests that the ion migration occurs quickly once the light is turned on. This time scale also explains the photo-current hysteresis in perovskite solar cells, since each scanning point corresponds to a quick ion redistribution.

The ion conductivity is determined by the product of the ion migration velocity and ion concentration, while both of these follow the Arrhenius thermal-activation function. Therefore, the derived activation energy includes activation energies of both ion generation (concentration) and ion movement (mobility). To further estimate the ion migration activation energy, we directly measured the ion diffusion under illumination. Fig. 4a depicts the experiment setup which also visualized the accelerated bromide diffusion in triiodide perovskite under illumination. $PbBr_2$ particles were dispersed on top of $MAPbI_3$ polycrystalline films, with an average grain size of 300 nm, or single crystals, and energy-dispersive X-ray spectroscopy (EDS) was used to reveal Br element diffusion in the triiodide perovskite samples. Fig. 4b and d show typical SEM images of the samples, where a $PbBr_2$ particle with a size of 2–5 μm was clearly observed at the center of the image. The samples were either illuminated under 1 Sun conditions or kept in the dark at room temperature for 2 hours. After that, EDS mapping and line scanning were used to reveal the Br diffusion. Here, $PbBr_2$, rather than PbI_2, was chosen to reveal the halide migration to give an element contrast to be observed by EDS. Fig. 4c and e show the corresponding Br element mapping of the sample kept in the dark and after illumination for 2 hours, respectively. The Br element EDS image had a sharp edge for the $PbBr_2$ particle for the sample kept in the dark, and became blurred for the sample under illumination, which is direct evidence for the light enhanced diffusion of Br ions, because no bias was applied here. The element distribution can be seen more clearly from the element line scanning shown in Fig. 4f. These results revealed that light can enhance the ion diffusion in the perovskite polycrystalline film, which is not different from the light enhanced ion drifting process shown above. The ion diffusion activation energy can be derived from the ion mobility change under different temperatures, and the ion mobility can be calculated from the element distribution by the line scanning extracted from Fig. 4e. As shown in Fig. 4g, Br^- diffused a longer distance at a higher temperature of 50 °C than at room temperature (20 °C). We derived the Br diffusivity and

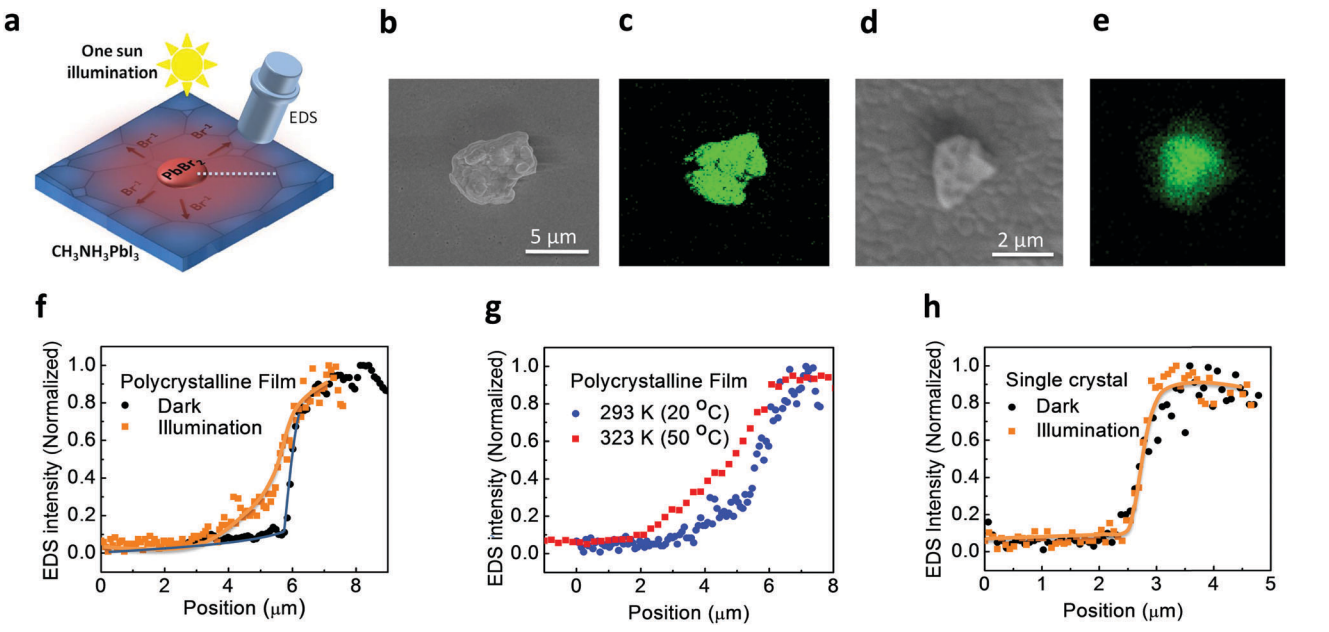

Fig. 4 EDS study of Br diffusion on $MAPbI_3$ film. (a) A schematic experimental setup for the ion diffusion study. (b and c) SEM and EDX Br-element distribution images of a $PbBr_2$ particle without illumination. (d and e) SEM and EDX Br-element distribution images of a $PbBr_2$ particle after illumination. (f and h) The line scan of the Br-element distribution on the $MAPbI_3$ polycrystalline film and $MAPbI_3$ single crystal without or with illumination. (g) The line scan of the Br element on the polycrystalline film under illumination at 293 K and 323 K.

activation energy by following the classical diffusion equations derived from Fick's laws.[29] The ion diffusivities were derived to be 1.7×10^{-12} cm^2 s^{-1} at RT and 3.1×10^{-12} cm^2 s^{-1} at 50 °C, which correspond to ion mobilities of 0.65×10^{-10} cm^2 V^{-1} s^{-1} at RT and 1.1×10^{-10} cm^2 V^{-1} s^{-1} at 50 °C, respectively. Then, the activation energy of Br^- diffusivity was calculated to be 0.17 eV. On the other hand, no Br^- diffusion could be observed on the $MAPbI_3$ single crystals even without any coverage. The EDS line scanning study of Br distribution was conducted on $MAPbI_3$ single crystal samples by following the same procedure as on the perovskite films, the results of which are shown in Fig. 4h. No obvious Br diffusion was detected in the single crystal samples even after the sample was illuminated under 1 Sun for 2 days (Fig. S1, ESI†). This can be explained by the high conductivity activation energy of ~0.47 eV measured in the single crystal samples under illumination in Fig. 2d. The represented small ion mobility in single crystals leads to the Br^- diffusion distance being too small to be detected by EDS, even after we increased the illumination time to two days. Although no Br diffusion was detected on single crystals, we could still estimate the lower limit of the ion mobility activation energy. We assumed that the Br^- diffusion distance after 48 hours of illumination was less than 0.1 μm, the value of which is based on the spatial resolution of the state-of-art EDS/SEM facility.[34] The upper limit of mobility was calculated to be 2.2×10^{-14} cm^2 V^{-1} s^{-1}, which is four orders of magnitude smaller than that in polycrystalline films. Then, the lower limit of the mobility activation energy was calculated to be 0.38 eV. This study also points to a means to suppress ion migration, which could induce device instability in the long term, though ion migration has been demonstrated by us to enhance device efficiency in the short term.[10] Thus increasing the grain size to minimize the ion drift channels such as the grain boundaries is a practical and effective way to decrease the ion migration and increase the device's light stability. Increasing grain size thus not only increases the efficiency of perovskite solar cells by reducing the charge recombination at GBs,[35,36] but also enhances their stability by reducing ion migration along GBs.

Conclusions

In conclusion, we have studied the effect of light on the ion migration of organic–inorganic hybrid perovskite films and single crystals. For a small grain film, the activation energy under light is only 0.08 eV compared with 0.27 eV in the dark. The greatly reduced activation energy is also found in a larger grain sample, a single crystal and a PMMA covered sample, demonstrating a common characteristic of light-promoted ion movement. The ion drift velocity for the $CH_3NH_3PbI_3$ film under 1 Sun illumination is more than an order of magnitude higher than that in dark. We also observed a wider Br distribution at the edge of the $PbBr_2$ particle in striking contrast with an undetectable edge change in the dark. In most solar cells, it is possible that ions start to migrate once the device is exposed to light and the migration could be finished within subseconds. A large quantity of ion migration and accumulation at contacts may impair the device efficiency and stability. Therefore minimizing the available ion channels and increasing the grain size is an effective way to enhance the device stability, which is in line with the objective of enhancing device stability. This work could have profound significance for the improvement of photovoltaic performance of the material and opens up a possibility of developing a new light-controlled solid electrolyte or memory device.

Experimental section

Device fabrication

The lateral $MAPbI_3$ device was fabricated on a glass substrate. At first, a 300 nm thick $MAPbI_3$ film was spin coated on glass with a two-step interdiffusion method. In particular, PbI_2 (40 wt%) and MAI (4.0 wt%) were first dissolved in dimethylformamide and 2-propanol, respectively, to form precursor solutions. The PbI_2 hot solution was spun onto glass at 6000 rpm. Then, the hot MAI solution was spin coated on PbI_2 film at 6000 Hz for 35 s. The bilayer films were then annealed at 100 °C for 1 h. The perovskite film with a larger grain size was fabricated using solvent annealing. Then, 50 nm Au electrodes with spacing of 50 μm were thermally deposited using a shadow mask. For the PMMA covered film, PMMA (15%) was spun onto the film at 4000 rpm and then was annealed at 100 °C for 10 minutes. The $MAPbI_3$ single crystal was prepared by slowly cooling down the supersaturated precursor solution from 110 to 60 °C with a cooling rate of approximately 0.1–0.5 °C h^{-1}. The resulting crystals were separated from the mother solution, and then washed with diethyl ether and isopropyl alcohol.

Film and device characterization

The current was extracted at 60 s after the voltage source was switched on. The measurements were performed in a Lakeshore Probe Station under a vacuum of 10^{-5} Pa with white light through a quartz window. The samples were placed on a copper plate with its temperature being controlled by a heater and injected liquid N_2, and this varied from 77 K to 350 K. A high voltage supply (Keithley 240a) with a maximum voltage output of 1200 V was used for the poling process. A semiconductor analyzer (Keithley 4200) was used for the current measurement. We firstly cooled the device to 110 K and then stabilized it at 110 K for 0.5 hour. Subsequently the device was heated to an objective temperature and stabilized at the temperature for 5 minutes before the current measurement was performed.

Energy-dispersive X-ray spectroscopy (EDS) study

The samples for the EDS study were fabricated by dispersing $PbBr_2$ particles on top of a perovskite film. The perovskite film fabrication followed the method described in the Device fabrication section. The $PbBr_2$ particles were dispersed in dichlorobenzene (DCB) solvent and spin-coated on top of the perovskite films. After that, the samples were kept in a glovebox at room

temperature for 1 hour to evaporate the DCB solvent. Then, the samples were kept under dark conditions or illuminated under 1 Sun conditions for 2 hours. The EDS line scanning was carried out on a FEI Nova NanoSEM 450 instrument equipped with an Oxford X-MAX energy dispersive X-ray spectroscope. The typical electron acceleration voltage for X-ray excitation was 10 kV.

Computational details

All the related physical formulas and computation details are included in the ESI.†

Acknowledgements

This work is financially supported by National Science Foundation (DMR-1505535 and ECCS-1252623). J. Xing acknowledges the support of the visiting professor award from China Scholarship Council and Fundamental Research Funds for the Central University (Grant No. 53200859478 and 53200859128).

References

1 S. D. Stranks, G. E. Eperon, G. Grancini, C. Menelaou, M. J. Alcocer, T. Leijtens, L. M. Hertz, A. Petrozza and H. J. Snaith, *Science*, 2013, **342**, 341.
2 C. Wehrenfennig, G. E. Eperon, M. B. Johnston, H. J. Snaith and L. M. Hertz, *Adv. Mater.*, 2014, **26**, 1584.
3 M. A. Green, A. Ho-Baillie and H. J. Snaith, *Nat. Photonics*, 2014, **8**, 506.
4 M. A. Green, Y. Jiang, A. M. Soufiani and A. Ho-Baillie, *J. Phys. Chem. Lett.*, 2015, **6**, 4774.
5 Q. Dong, Y. Fang, Y. Shao, P. Mulligan, J. Qiu, L. Cao and J. Huang, *Science*, 2015, **347**, 967.
6 A. Kojima, K. Teshima, Y. Shirai and T. Miyasaka, *J. Am. Chem. Soc.*, 2009, **131**, 6050.
7 http://www.nrel.gov/solar/news/2016/46060.
8 W. Tress, N. Marinova, T. Moehl, S. M. Zakeeruddin, M. K. Nazeeruddin and M. Gratzel, *Energy Environ. Sci.*, 2015, **8**, 995.
9 Z. Xiao, Y. Yuan, Y. Shao, Q. Wang, Q. Dong, C. Bi, P. Sharma, A. Gruvermann and J. Huang, *Nat. Mater.*, 2015, **14**, 193.
10 Y. Deng, Z. Xiao and J. Huang, *Adv. Energy Mater.*, 2015, **5**, 1500721.
11 E. T. Hoke, D. J. Slotcavage, E. R. Dohner, A. R. Bowring, H. I. Karunadasa and M. D. McGehee, *Chem. Sci.*, 2015, **6**, 613.
12 E. J. Juarez-Perez, R. S. Sanchez, L. Badia, G. Garcia-Belmonte, Y. S. Kang, I. Mora-Sero and J. Bisquert, *J. Phys. Chem. Lett.*, 2014, **5**, 2390.
13 Y. Zhao, J. Wei, H. Li, Y. Yan, W. Zhou, D. Yu and Q. Zhao, *Nat. Commun.*, 2016, **7**, 10228.
14 W. Nie, J.-C. Blancon, A. J. Neukirch, K. Appavoo, H. Tsai, M. Chhowalla, M. A. Alam, M. Y. Sfeir, C. Katan, J. Even, S. Tretiak, J. J. Crochet, G. Gupta and A. D. Mohite, *Nat. Commun.*, 2016, **7**, 11574.
15 Y. Yuan, J. Chae, Y. Shao, Q. Wang, Z. Xiao, A. Centrone and J. Huang, *Adv. Energy Mater.*, 2015, **5**, 1500615.
16 D. W. deQuilettes, W. Zhang, V. M. Burlakov, D. J. Graham, T. Leijtens, A. Osherov, V. Bulovic, H. J. Snaith, D. S. Ginger and S. D. Stranks, *Nat. Commun.*, 2016, **7**, 11683.
17 C. Eames, J. M. Frost, P. R. F. Barnes, B. C. O'Regan, A. Walsh and M. S. Islam, *Nat. Commun.*, 2015, **6**, 7497.
18 J. Haruyama, K. Sodeyama, L. Han and Y. Tateyama, *J. Am. Chem. Soc.*, 2015, **137**, 10048.
19 Y. Zhou, L. You, S. Wang, Z. Ku, H. Fan, D. Schmidt, A. Rusydi, L. Chang, L. Wang, P. Ren, L. Chen, G. Yuan, L. Chen and J. Wang, *Nat. Commun.*, 2016, **7**, 11193.
20 Y. Yuan, Q. Wang, Y. Shao, H. Lu, T. Li, A. Gruverman and J. Huang, *Adv. Energy Mater.*, 2016, **6**, 1501803.
21 C. Bischoff, K. Schuller, S. P. Beckman and S. W. Martin, *Phys. Rev. Lett.*, 2012, **109**, 075901.
22 J. B. Goodenough, *Rep. Prog. Phys.*, 2004, **67**, 1915.
23 Q. Wang, Q. Dong, T. Li, A. Gruverman and J. Huang, *Adv. Mater.*, 2016, **28**, 6734.
24 Y. Shao, Y. Yuan and J. Huang, *Nat. Energy*, 2016, **1**, 15001.
25 Z. Xiao, Q. Dong, C. Bi, Y. Shao, Y. Yuan and J. Huang, *Adv. Mater.*, 2014, **26**, 6503.
26 J. Liu, C. Gao, X. He, Q. Ye, L. Ouyang, D. Zhuang, C. Liao, J. Mei and W. Lau, *ACS Appl. Mater. Interfaces*, 2015, **7**, 24008.
27 J. Lian, Q. Wang, Y. Yuan, Y. Shao and J. Huang, *J. Mater. Chem. A*, 2015, **3**, 9146.
28 Y. Shao, Y. Fang, T. Li, Q. Wang, Q. Dong, Y. Deng, Y. Yuan, H. Wei, M. Wang, A. Gruverman, J. Shield and J. Huang, *Energy Environ. Sci.*, 2016, **9**, 1752.
29 D. A. Porter, K. E. Easterling and M. Y. Sherif, *Phase transformations in metals and alloys*, 3rd edn, 2009.
30 Y. Yuan and J. Huang, *Acc. Chem. Res.*, 2016, **49**, 286.
31 A. B. Munoz-Garcia, A. M. Ritzmann, M. Pavone, J. A. Keith and E. A. Carter, *Acc. Chem. Res.*, 2014, **47**, 3340.
32 A. Buin, P. Pietsch, J. Xu, O. Voznyy, A. H. Ip, R. Comin and E. H. Sargent, *Nano Lett.*, 2014, **14**, 6281.
33 R. Gottesman, E. Haltzi, L. Gouda, S. Tirosh, Y. Bouhadana and A. Zaban, *J. Phys. Chem. Lett.*, 2014, **5**, 2662.
34 S. Burgess, X. Li and J. Holland, *Microsc. Anal.*, 2013, **6**, S8.
35 C. Bi, Q. Wang, Y. Shao, Y. Yuan, Z. Xiao and J. Huang, *Nat. Commun.*, 2015, **6**, 7747.
36 Y. Bi, E. M. Hutter, Y. Fang, Q. Dong, J. Huang and T. J. Savenije, *J. Phys. Chem. Lett.*, 2016, **7**, 923.

